

**Effect of thermal conductivity on phased array imaging of closed crack by global preheating and local cooling**

広域加熱・局所冷却による閉じたき裂のフェーズドアレイ映像化における熱伝導率の影響

Koji Takahashi<sup>1,‡</sup>, Kouki Ohmachi<sup>1</sup>, Kentaro Jinno<sup>1</sup>, Yoshikazu Ohara<sup>1</sup> and Kazushi Yamanaka<sup>1</sup> (<sup>1</sup>Tohoku Univ.)

高橋 恒二<sup>1,‡</sup>, 大町 弘毅<sup>1</sup>, 神納 健太郎<sup>1</sup>, 小原 良和<sup>1</sup>, 山中 一司<sup>1</sup> (<sup>1</sup>東北大)

**1. Introduction**

In an aluminum alloy of airplanes and a stainless steel of power plants, crack closure is a critical issue that causes the overlook or underestimation of cracks. As a method for measuring closed crack depths, a closed-crack imaging method, the subharmonic phased array for crack evaluation (SPACE)<sup>1-3</sup> has been demonstrated. On the other hand, a crack opening method, global preheating and local cooling (GPLC)<sup>4-6</sup> has recently been proposed. So far, a closed fatigue crack depth was accurately measured in an aluminum-alloy specimen and a crack closure stress estimation method was demonstrated. However, the effect of thermal conductivity on GPLC has not been examined.

In this study, we study the applicability of GPLC for aluminum alloy and stainless steel with different thermal conductivities. We first examine the thermal stress change with a cooling time, based on analytical solutions. Subsequently, we examine the change in crack depths in linear phased array (PA) images with a cooling time.

**2. Principle of GPLC**

A schematic of GPLC is shown in Fig. 1. After GP and before LC, an open crack is imaged by PA [Fig. 1(a)], whereas a closed crack is not imaged. Subsequently, the top surface of the specimen is locally cooled by cooling sprays. The vicinity of the top surface thermally contracts, and thereby, a tensile thermal stress is applied to the closed crack by a principle similar to that of a three-point bending test. Here, the applied stress can be controlled by varying the GP temperature since the stress depends on the temperature distribution within the specimen. Thus, the closed crack tip is opened and thereby, it is imaged by PA [Fig. 1(b)].

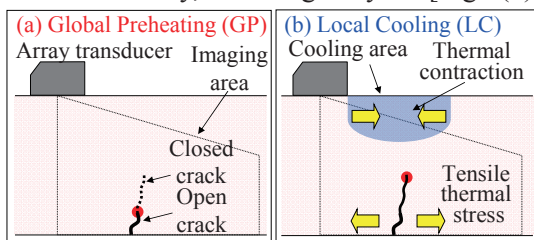


Fig. 1 Schematics of GPLC.

**3. Analysis of thermal stress induced by GPLC**

To examine the effect of thermal conductivity on GPLC, we analyzed the thermal stress. Assuming the boundary condition of the third kind with a fixed heat transfer coefficient  $h$  on the top surface and a semi-infinite solid, the internal temperature distribution  $T(z, t)$  is given by<sup>7)</sup>

$$T(z, t) = (T_\infty - T_i) \left\{ \operatorname{erfc} \left( \frac{z}{2\sqrt{at}} \right) - \exp \left( \frac{hz}{k} + \frac{h^2 at}{k^2} \right) \operatorname{erfc} \left( \frac{z}{2\sqrt{at}} + \frac{h\sqrt{at}}{k} \right) \right\} + T_i, \quad (1)$$

where  $T_\infty$  is the cooling temperature due to LC,  $T_i$  is the GP temperature,  $k$  is the thermal conductivity, and  $a$  is the thermal diffusivity.

Assuming the specimen as a plate, the thermal bending stress  $\sigma(z, t)$  is given by<sup>8)</sup>

$$\sigma(z, t) = \frac{12\alpha Ez}{H^3(1-\nu)} \int_{-\frac{H}{2}}^{\frac{H}{2}} T(z, t) dz, \quad (2)$$

where  $\alpha$  is the coefficient of linear expansion,  $E$  is Young's modulus, and  $\nu$  is Poisson's ratio.

Based on Eqs. (1) and (2) with the parameters listed in Tables I and II, we calculated the thermal stresses at crack tips in A7075 and SUS316L (Fig. 2). In A7075,  $\sigma$  took a maximum at  $t=4-6$  s, and thereafter, gradually decreased. In SUS316L,  $\sigma$  monotonically increased with  $t$ . This is because the large temperature difference between the top surface and crack area continued for a longer time in SUS316L than in A7075. Thus, we found that, to increase the maximal  $\sigma$ , the increase in the cooling time is sufficient in SUS316L, although the increase in the GP temperature is required in A7075.

Table I. Physical properties of A7075 and SUS316L<sup>9)</sup>

	$k$ [W/(m·K)]	$a$ [m <sup>2</sup> /s]	$\alpha$ [1/K]	$E$ [GPa]	$\nu$ [-]
A7075	130	$4.8 \times 10^{-5}$	$23.4 \times 10^{-6}$	71	0.33
SUS 316L	16.3	$8.4 \times 10^{-5}$	$15.9 \times 10^{-6}$	193	0.30

Table II. Parameters used for analysis

$T_\infty$ [K]	$T_i$ [K]	$h$ [W/(m <sup>2</sup> · K)]
218	323	$2.0 \times 10^4$

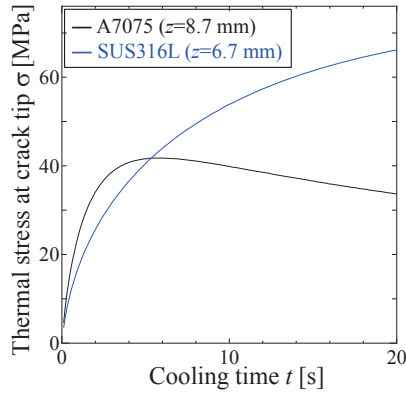


Fig. 2 Thermal stresses at crack tips in A7075 and SUS316L.

#### 4. Experiment

In this experiment, we used A7075 (fatigue crack depth 11.3 mm) and SUS316L (13.3 mm) compact tension (CT) specimens. In GPLC, after globally preheating (GP) the specimen to 323 K on a hotplate, the top surface was locally cooled (LC) by two cooling sprays (-218 K) for 20 s. During the LC, we monitored the cracks by PA using a PZT array transducer (5 MHz, 32 el.).

For each specimen, the snapshots of the PA images during GPLC are shown in Figs. 3 and 4. In A7075, before LC, the closed crack was not imaged in Fig. 3(a), whereas at (b)  $t=5$  s, the crack was clearly observed and the measured depth was the same as the true one of 11.3 mm. Then, at (c)  $t=10$  s and (d)  $t=20$  s, the crack depth decreased.

In SUS316L, before LC, the crack depth was 7.2 mm in Fig. 4(a), whereas at (b)  $t=5$  s, (c)  $t=10$  s, and (d)  $t=20$  s, the measured crack depth of 13.1 mm was almost the same as the true one of 13.3 mm. Thus, we demonstrated that GPLC is useful in measuring the closed crack depth for both materials with different thermal conductivities.

The crack depths were measured in the PA images as a function of cooling time (Fig. 5). In SUS316L, The maximal crack depth continued until  $t=20$  s. On the other hand, in A7075, the crack depth gradually decreased after  $t=8$  s. It qualitatively agreed with the analytical results (Fig. 2). In terms of the duration showing the maximal crack depth, it was 17 s ( $t=3-20$  s) in SUS316L, whereas it was 4 s ( $t=4-8$  s) in A7075. This shows that the measurement of closed crack depth is easier in SUS316L than in A7075.

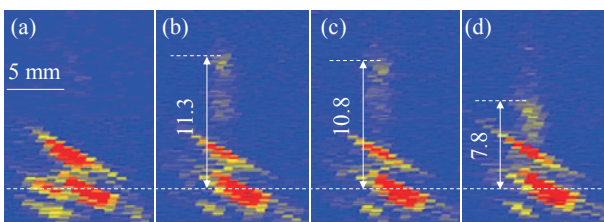


Fig. 3 PA images during GPLC in A7075: (a)Before LC, (b) $t=5$  s, (c) $t=10$  s, (d) $t=20$  s.

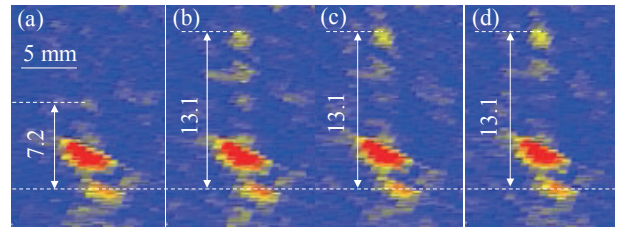


Fig. 4 PA images during GPLC in SUS316L: (a)Before LC, (b) $t=5$  s, (c) $t=10$  s, (d) $t=20$  s.

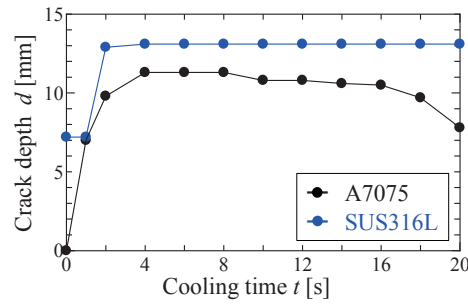


Fig. 5 Comparison of crack depths with  $t$  between A7075 and SUS316L.

#### 5. Conclusions

To examine the applicability of GPLC for A7075 and SUS316L with different thermal conductivities, we theoretically examined thermal stress changes with cooling time during GPLC. As a result, we found that the thermal stress changes depending on the thermal conductivity. In experiment, the closed crack depth was accurately measured in both materials. Furthermore, the change in crack depths with cooling time qualitatively agreed with the analytical results. We also found that the measurement of closed crack depth is easier in SUS316L than in A7075. Thus, we showed that the thermal stress analysis is useful in examining the effect of thermal conductivity on GPLC and in selecting an appropriate experimental condition.

#### References

- 1) Y. Ohara, et al., *App. Phys. Lett.*, **90** (2007) 011902.
- 2) Y. Ohara, et al., *Jpn. J. App. Phys.*, **47** (2008) 3908.
- 3) Y. Ohara, et al., *Jpn. J. App. Phys.*, **48** (2009) 07GD01.
- 4) Y. Ohara, et al., *App. Phys. Lett.*, **103** (2013) 031917.
- 5) Y. Ohara, et al., *Mater. Trans.*, **55** (2014) 1003.
- 6) K. Takahashi, et al., *Jpn. J. App. Phys.*, **53** (2014) 07KC20.
- 7) F. P. Incropera, et al., *Introduction to Heat Transfer* (Wiley, New York, 2007) p. 286.
- 8) S. P. Timoshenko, et al., *Theory of Elasticity* (McGraw-Hill, New York, 1951) p. 403.
- 9) E. A. Brandes, et al., *Smithells Metals Reference Book* (Butterworth-Heinemann, London, 1992) p. 14.